PROCEEDINGS OF SCIENCE

Measurements of ^{12}C ions fragmentation cross sections on a thin gold target with the FIRST apparatus

Marco Toppi, on behalf of the FIRST collaboration*
Istituto Nazionale di Fisica Nucleare-Laboratori Nazionali di Frascati, Frascati, Italy
E-mail: marco.toppi@lnf.infn.it

The FIRST (Fragmentation of Ions Relevant for Space and Therapy) experiment at the Helmholtz Center for Heavy Ion research (GSI) was designed and built by an international collaboration from France, Germany, Italy and Spain in order to perform precise measurements of the fragmentation cross sections of a ^{12}C ion beam with different thin targets. In particular the experiment main purpose is to measure the double differential cross sections of the fragmentation of a ^{12}C beam in the energy range of 100-1000 MeV/nucleon, measured as a function of the emitted fragment angle and kinetic energy.

Such energy range is of great interest in the fields of ion therapy for the treatment of tumors and of space radioprotection. In particular the cosmic ray spectrum for ^{12}C ions presents a peak in this energy range, while the maximum energy usable in ion therapy treatments with carbon ions is 400 MeV/nucleon. Accurate fragmentation cross section measurements are needed to validate the interaction nuclear models implemented in Monte Carlo codes useful to develop radiation treatment planning for tumor therapy and particle transport codes in shielding materials to estimate health risks for human missions in space.

The FIRST scientific program start was on summer 2011 and was focused on the measurement of 400 MeV/nucleon ^{12}C beam fragmentation on a 0.5 mm gold target (4.5×10^6 events were collected). This paper presents the relative analysis, the developed Monte Carlo simulation, the implemented reconstruction algorithms and the obtained results in terms of differential fragmentation cross sections C-Au, measured as a function of the fragment angle and kinetic energy, in the forward angular region ($\theta \lesssim 6^\circ$).

54th International Winter Meeting on Nuclear Physics
25-29 January 2016
Bormio, Italy

*Speaker.

PoS(BORMIO2016)035

1. Introduction

The study of the nuclear fragmentation processes occurring in the interaction of highly energetic ions in matter is of great interest both in basic research (e.g. to improve the understanding of hadronic showers development in the atmosphere) and in applied physics, in particular in cancer therapy and space radiation protection fields [1, 2]. Accurate measurements of fragmentation cross sections of light ions interacting with elemental and composite targets are crucials to benchmark and improve the nuclear interaction models implemented in Monte Carlo (MC) simulation codes. In order to provide the necessary experimental input to MC simulations, a small set of measurements can be used: the interpolation of cross sections for different energies and target materials composition allows, starting from a selected number of target/energy combinations, to build a model covering all the application needs.

The current agreement between predictions of nuclear interaction models implemented in MC codes and experimental data is encouraging but there is still room for improvement, mainly due to the lack of available data and to their limited precision [3]. So far, only yields or total and partial charge-changing fragmentation cross sections have been measured with high precision and in a variety of target and beam energy configurations. However the most valuable results, the double differential cross section (DDCS) measurements, that would allow a stringent test of the nuclear model predictions, are still missing. In particular, while the fluences and the total cross sections are currently well described, the production of light fragments and their angular distribution is affected by large uncertainties and different algorithms are predicting yields that can differ up to an order of magnitude. The NASA completed a survey of a large data base [2] of measured nuclear fragmentation cross sections including approximately 50000 data sets, and concluded that several experimental data are missing: accurate measurements of DDCS of light ions in the energy range 100 - 1000 MeV/nucleon are, hence, urgently needed to improve nuclear interaction models and are also of great interest in the fields of ion therapy for the treatment of tumors and of space radioprotection.

The FIRST (Fragmentation of Ions Relevant for Space and Therapy) experiment, at the SIS accelerator of GSI laboratory in Darmstadt, has been designed to perform precise measurements of the DDCS, with respect to the angle and energy of the emitted fragment, of a ^{12}C ion beam in the energy range 100 - 1000 MeV/nucleon with different thin targets [4]. In this contribution we present the analysis of data collected with the FIRST apparatus using a ^{12}C beam of 400 MeV/nucleon impinging on a 0.5 mm gold target [5]. The experimental setup was optimized to study two distinct angular regions: the small angle region (subject of this contribution), where fragments are produced with a polar angle θ with respect to the impinging beam direction (z axis) smaller than 6° and a large angle region with $6° < \theta < 40°$. The analysis techniques used for the fragments reconstruction in the forward angular region and the results of the elemental and isotopic single differential cross sections with respect to fragment angle and energy will be discussed.

2. The FIRST apparatus

The FIRST apparatus, shown in Fig.1, is composed of several sub detectors optimized for the detection of all the charged fragments produced by the interaction of a ^{12}C ion with the target up

to a maximum aperture angle of 40° with respect to the beam axis. A ^{12}C ion, before interacting with the target (TG), as a first step, impinges on the start counter (SC), a thin scintillator that monitors the number of ^{12}C ions in the beam, provides the trigger of the experiment and start the Time of Flight (ToF) measurement. Afterwards the beam goes through the Beam Monitor (BM), a drift chamber that measures the direction and the impact point on the target [6]. The fragmentation vertex produced in the interaction with the target is reconstructed with a silicon pixel detector (VTX), located just after the target, that has a track angular acceptance of $\theta = 40°$ [7]. The forward fragments produced with polar angle $\theta \lesssim 6°$ enter in the angular acceptance of the ALADIN (A Large Acceptance DIpole magNet) dipole magnet [4, 5]. The trajectory and the rigidity (momentum over charge ratio, pc/Z) of such fragments are reconstructed using the magnetic bending provided by the magnet in the x-z plane, and by matching the fragments position on the ToF-Wall (TW), a large area hodoscope formed of two scintillators layers [4, 5].

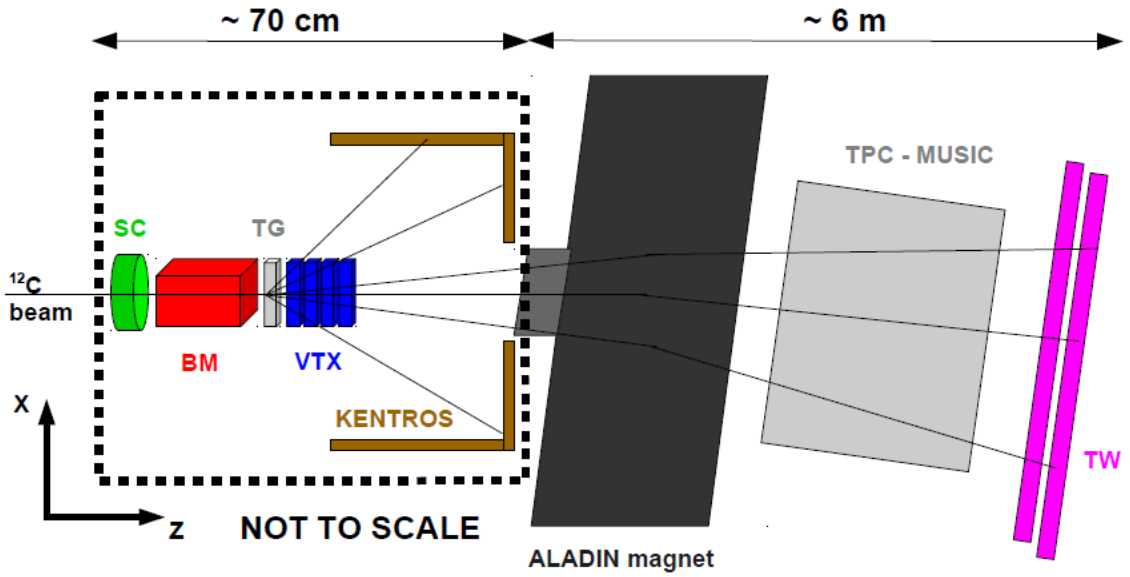

Figure 1: Schematic view of the FIRST detector set up. The lines show the path of the fragments produced in the target (TG). The detectors in the interaction region are a start counter (SC), a beam monitor (BM) a vertex detector (VTX) and a thick scintillator system (KENTROS). The fragments tracks bended by the ALADIN magnet are detected by the ToF-Wall (TW), a large area hodoscope of two walls of scintillator detectors

The large volume time projection chamber (TPC-MUSIC [4]), was placed after the ALADIN magnet and before the TW, aiming at the measures of track directions and energy releases, but could not be operated during the data taking due to an anomalous increase of the current in the main cathode.

The VTX and the TW detectors are the only two available detectors able to perform the cross section measurement for the forward emitted fragments in the angular acceptance of the ALADIN magnet ($\theta \lesssim 6°$) and for this reason will be described in detail in the next paragraphs § 2.1 and § 2.2. The tracking algorithm uses an iterative procedure that matches the VTX tracks and the TW hits

detected in each event: special care is needed while performing the extrapolation from the VTX to the far away ($\sim$ 6 m) TW.

The fragments emitted outside the angular acceptance of the ALADIN magnet, mainly light ions (p, d, t, ^{3}He and ^{4}He), are detected by KENTROS (Kinetic ENergy and Time Resolution Optimized on Scintillator [4]), a thick scintillators system organized in a cylindrical shape. The analysis described in this paper is focused on the measurement of the differential cross sections for forward peaked fragments emitted in the magnet angular acceptance. For this reason the KENTROS detector is not used in the following analysis.

2.1 The Vertex Detector

The Vertex detector (VTX) is a silicon pixel detector placed immediately after the target along the beam direction and used to measure the trajectory of charged particles coming out from the target.The VTX is composed of four layers each consisting of two MIMOSA-26 (M26) silicon pixel sensors [8] glued on the two sides of a printed circuit board (PCB), as shown in Fig. 2 (left). The sensitive area of each sensor is 10.6 mm $\times$ 21.2 mm covered by 576 rows and 1152 columns of pixels with 18.4 μm pitch. The thickness of about 50 μm per sensor allows to minimize the lateral straggling of the impinging particles and to reduce the secondary fragmentation inside the sensor at a level of a few per cent, with respect to the on-target one.

The energy deposited by a ionizing particle impinging a M26 sensor produces charge carriers that are collected by a number of adjacent pixels that form a cluster. The off-line VTX detector data processing starts from the raw data file reading, from which a list of fired pixel is extracted. The VTX reconstruction software [7], consisting of three different algorithms, gathers the fired pixels to identify cluster in each plane (*clustering*), builds tracks with aligned clusters on different planes (*tracking*) and estimates the vertex position from reconstructed tracks (*vertexing*). For each reconstruction step at least two algorithms, providing consistent results, have been implemented [7]. Only the faster algorithm and with a lower fakes number has been chosen as default for each step. The alternative algorithms have been used to assign systematic uncertainties. Each of these algorithms have shown a high reconstruction efficiency greater than 99% [7]. An excellent tracking resolution ($<$ 10 μm) and vertexing resolution ($<$ 10 μm) have been measured in the x-y plane (see [5]).

2.2 The ToF-Wall detector

The ToF-Wall (TW) detector is a large area hodoscope (1.10 m long and 2.40 m wide) made of two scintillators layers placed $\simeq$ 6 m far from the target, along the trajectory of the ^{12}C beam, beyond the TPC (Fig. 1). Each layer consists of BC-408 plastic scintillator slats (vertical bars 110 cm long, 1 cm thick, 2.5 cm wide), divided in 12 modules of 8 slats each, for a total number of 192 independent scintillators. The two scintillators walls are separated by 8 cm from each other: the plane closest to the magnet is called "front wall", while the other one "rear wall". A picture of the TW detector layout is shown in Fig. 2 (right).

The light produced by a charged track impinging on a TW slat is collected at the top and at the bottom of the slat by two R3478 Hamamatsu PMT. The analog signal from each PMT is split into two branch of the acquisition chain. The first branch consists of a FastBus ADC (model Lecroy

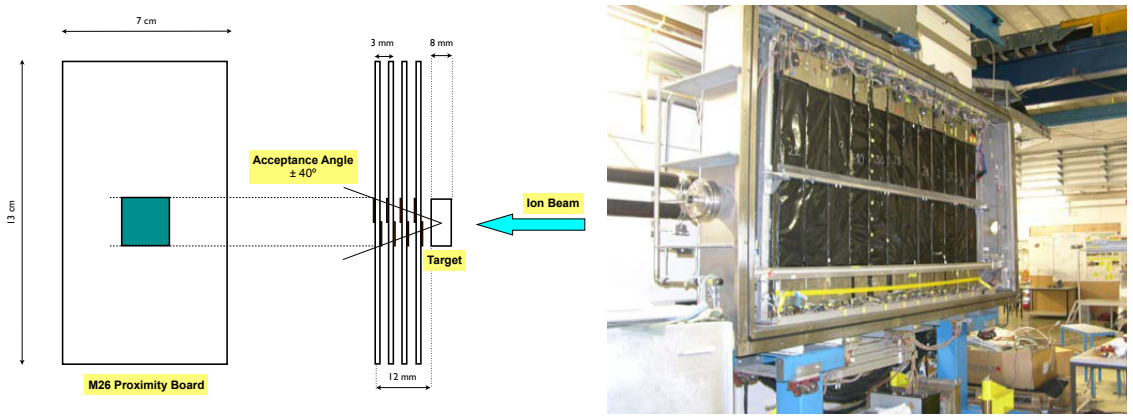

Figure 2: On the left: Sketch of the VTX detector arrangement: following the target the four PCB planes, each housing the two M26 sensors, one on each side are visible. The M26 sensors are placed over a square hole in the PCB itself obtaining an active volume of 2×2 cm^2. On the right: Picture of the TW detector: the 12 modules of the front wall are clearly visible

1885F) that provides the energy information exploiting the measurement of the ionization released by the impinging particle. The second branch of the electronic chain consist of a CFD (Constant Fraction Discriminator), a digital delay module and a TDC (model Lecroy 1875) that provides the time information. Combining such informations the energy loss (E_{loss}), the arrival time and the vertical impact position y of the track can be reconstructed. Moreover, the slat number gives the information about the horizontal position (x coordinate) of the TW hit, with a resolution limited by the slat width to $\sigma_X \lesssim 2.5$ cm$/\sqrt{12}$, and also about the fired wall (i.e. z coordinate). The fragment charge is reconstructed by combining the E_{loss} measurements with the start time from SC and the arrival time of the TW, that provide together the ToF of the particle (see § 2.3).

The resolutions of the physical quantities (E_{loss}, y, ToF), reconstructed by the TW, are estimated using tracks for which both hits in the front and in the rear wall are recorded. Both hits have to be compatible with the same track according to their position (slat number and y, within a certain tolerance) and their charge (see § 2.3). The distribution of the difference between the values measured for hits in the two planes is built for each charge. The resolutions are estimated from a Gaussian fit to such distributions and then used for the tuning of the Monte Carlo signal processing (see § 3). In general such resolutions are better for carbon than for hydrogen fragments (see [5]). The y coordinate resolution depends, as expected, on the value of the vertical coordinate itself and it range between 2 - 9 cm from carbon to hydrogen ions, while the energy resolutions range between 2 - 12 MeV. The ToF resolution is about 800 ps for all fragments.

2.3 Charge identification algorithms Z_{ID}

The particle charge is fundamental for the reconstruction of the momentum and of the mass of the track (see § 4). Two different algorithms, based on the information from TW and VTX have been developed to identify the fragment charge (see [5]). The TW charge identification algorithm (Z_{ID}) is based on the reconstructed quantities E_{loss} and ToF. The TW performances allow the discrimination of six spots in the E_{loss}-ToF plane, related to different fragment charges, as shown in

Fig. 3 (left): for each spot the Bethe-Bloch curve with the corresponding Z is superimposed. The TW Z_{ID} algorithm assigns to each point in the E_{loss}-ToF plane (a TW hit) the charge Z corresponding to the Bethe-Bloch curve that minimizes its distance from it.

A VTX Z_{ID} algorithm has been calibrated on data, using the measured cluster size for each charge from TW Z_{ID}: the correlation between these two quantities is shown in Fig. 3 (right). The values shown in Fig. 3 (right) are the Most Probable values (MPV) of Landau fits of the cluster size distributions for particle of different TW charges. For each reconstructed track, the VTX Z_{ID} algorithm compares the cluster size value with the calibrated Landau distributions in order to assign a probability for each Z hypothesis. The hypothesis with the largest probability is then used to assign the Z_{ID} to the fragment.

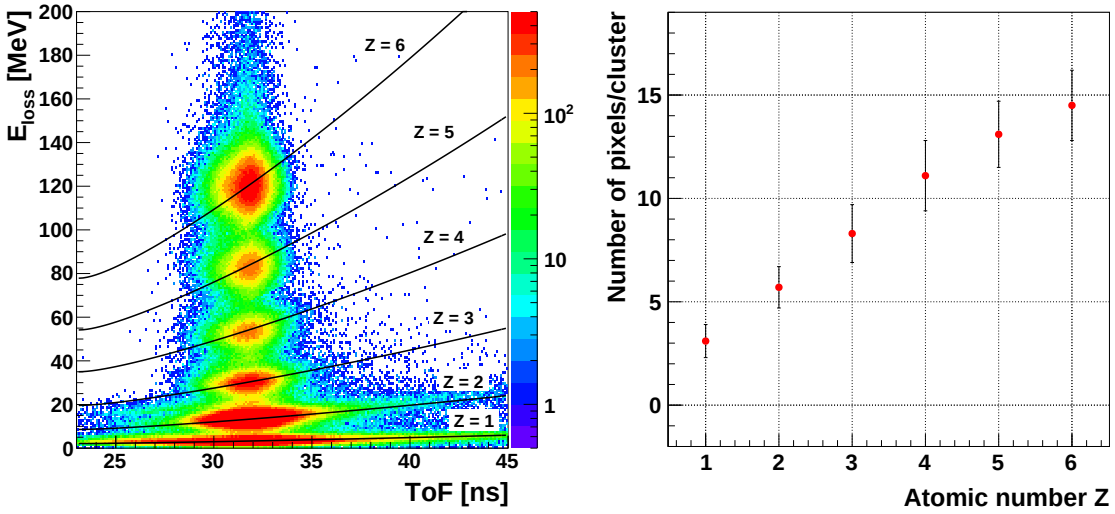

Figure 3: On the left: Measured E_{loss} vs ToF distribution, for all the TW hits reconstructed in the full data sample. The corresponding Bethe-Bloch curves, fitted on the data sample, are superimposed in black. On the right: VTX tracks mean cluster size (number of pixels per cluster) as a function of the fragment atomic number Z obtained by the TW.

3. The Monte Carlo simulation

The full simulation of the FIRST experiment has been implemented using the general purpose Monte Carlo code FLUKA [9]. A sample of 50 million MC events of ^{12}C ions interacting with a gold target are used for the analyses described in the following paragraphs. In particular MC simulation is needed for the optimization of the reconstruction algorithm and the evaluation of the efficiencies, angular end kinetic energy resolutions and for the background subtraction. For this purpose each reconstructed track is associated with a MC generated track and the reconstructed variables (kinetic energy, mass, charge, emission angle, momentum) are compared with the corresponding true value at generator level (see § 4).

4. The reconstruction algorithm

The global tracking algorithm implements three main steps (see [5]).

1. The global tracks are built by pairing the tracks reconstructed with the VTX and the hits detected by the TW. For all the preselected events, all the possible combinations of VTX tracks and TW hits are considered in such a way to produce a list of global tracks candidates: each VTX track matched with each TW hit can constitute a potential global track.

2. For each selected global track candidate the charge, the ToF and the final position (x, y, z) are measured by the TW, while the track origin position (x, y, z) and direction (θ and ϕ) before the magnet are provided by the VTX detector. Each candidate track is propagated from the target as a straight line towards the magnet, where the track is bended according to the Lorentz force differential equation in momentum p. A minimization algorithm, based on an initial momentum guess and on the Runge Kutta method for solving the Lorentz differential equation and providing the final momentum outside the magnet, determines the optimal value of pc/Z and the corresponding trajectory that matches the VTX track before the magnet and the TW x-position after the magnet. The particle path L can be determined from the trajectory. The particle momentum is determined multiplying the value of pc/Z from the tracking algorithm by the charge from the TW Z_{ID}. The particle velocity measurement is given by ToF and track path: $\beta = \frac{L}{\mathrm{ToF}\cdot c}$. The mass measured in the spectrometer is given by the ToF and momentum measurements: $Mc^2 = \frac{pc}{\beta\cdot\gamma}$ where γ is the Lorentz factor. The differential cross sections are measured in FIRST as a function of the fragment production angle (θ) with respect to the beam axis, measured using the tracks reconstructed by the VTX detector, and of the particle kinetic energy normalized to the mass number A, defined as: $\mathrm{E_{kin}} = \frac{1}{A}\left(\sqrt{p^2c^2+M^2c^4} - Mc^2\right)$.

3. The selection of the final tracks from the list of global tracks candidates is based on a scoring function that uses the quality of the match between VTX tracks and TW hits to select the best candidates. The scoring function is based on the difference Δ_y between the y coordinate measured by the TW and the y coordinate of the VTX track (y_{VTX}) extrapolated to the TW plane, and on the difference Δ_Z between the charges measured with the TW $\mathrm{Z_{ID}}$ and the VTX $\mathrm{Z_{ID}}$ algorithms. The adopted scoring function $S(\mathrm{y},\mathrm{Z})$, used for the track rating, is: $S(\mathrm{y},\mathrm{Z}) = \sqrt{\Delta_\mathrm{Z}^2\cdot\mathrm{W_Z^2} + \Delta_\mathrm{y}^2\cdot\mathrm{W_y^2}}$ where $\mathrm{W_y}$ and $\mathrm{W_Z}$ are two weighting factors. The weighting factors have been optimized using the full MC simulation and minimizing the fraction of wrong TW-VTX combinations. The pairing procedure can produce wrong VTX/TW hits matches, forming a random combination that is selected by the scoring algorithm. Such fragments are defined as "combinatorial background", since they represent the result of a reconstruction that artificially combines tracks and hits not belonging to a true fragment.

5. Tracking algorithm performances

The tracking algorithm performances have been validated using the MC simulation (see [5]). The angular and kinetic energy resolutions have been measured in order to evaluate possible bias

introduced by the reconstruction algorithm and to optimize the binning adopted for the cross section measurement.

The angular resolution σ_θ has been evaluated using global tracks from the full MC sample comparing the true fragment direction (θ_{true}) at the target exit point with the one reconstructed by the FIRST tracking algorithm (θ_{rec}). The angular resolution with respect to the track emission angle, for fragments and carbon ions is about $\sigma_\theta \sim 0.054^\circ$ for all fragments, except for hydrogens ions ($\sigma_\theta \sim 0.076^\circ$). Such numbers are entirely dominated by the intrinsic resolution of the VTX detector. The kinetic energy resolution ($\sigma_{\text{E}_{\text{kin}}}$) has been evaluated within the full MC simulation comparing the reconstructed energies with the corresponding true values at generator level. Fig. 4 (left) shows the E_{kin} resolution as a function of the measured kinetic energy. A rise of $\sigma_{\text{E}_{\text{kin}}}$ with respect to E_{kin} is observed for all fragments, as expected for a particle propagating in a magnetic field ($\sigma_{\text{p}}/p \propto p$).

The tracking efficiencies measured as a function of θ and E_{kin} are main ingredients to extract the differential cross sections as defined in next paragraph § 6. The tracking efficiencies have been evaluated, for each isotope coming from ^{12}C fragmentation, using the MC simulation sample, selecting only correct VTX-TW matches. For each fragment charge, the efficiency is defined as the ratio between the number of reconstructed tracks (n_{REC}) and the number of MC generated tracks (n_{PROD}) emerging from the target in the magnet angular acceptance: $\varepsilon_{\text{trk}} = \frac{\text{n}_{\text{REC}}}{\text{n}_{\text{PROD}}}$ The efficiency as a function of the measured angle θ is shown in Fig. 4 (right) for each isotope. The uncertainties shown are statistical only. The drop observed in the angular efficiency (Fig. 4, right) around 6° is due to the geometrical acceptance of the ALADIN magnet entrance window.

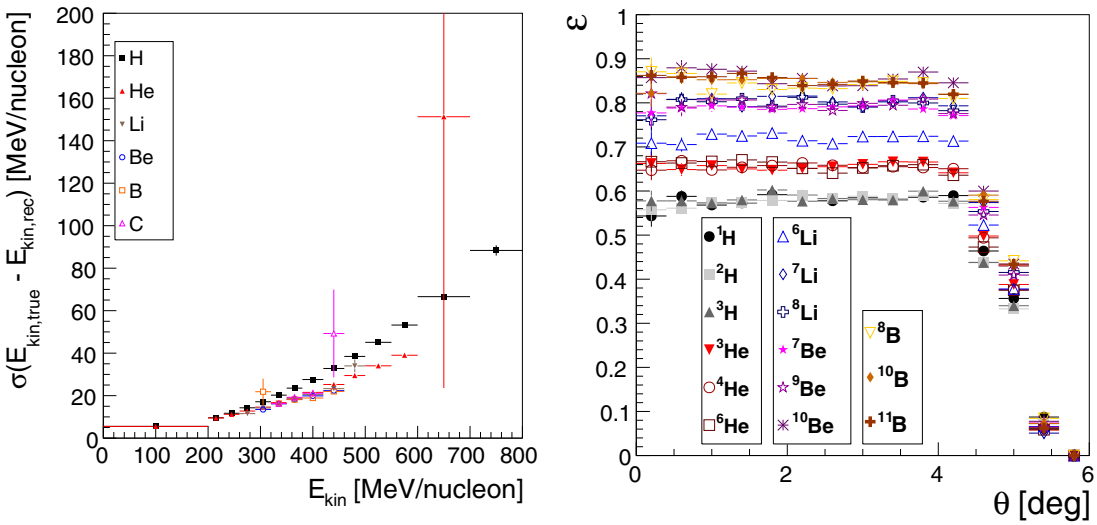

Figure 4: On the left: E_{kin} resolution for fragments with different Z_{ID}, from a global track MC sample selected requiring only correctly paired VTX tracks and TW hits. On the right: Tracking efficiency (ε_{trk}) for the identified isotopes as a function of fragment measured angle θ.

6. Cross section measurements

The differential fragmentation cross sections, with respect to the angle (θ) and to the normalized kinetic energy E_{kin}, for the production of the i-th isotope ${}^{A}_{Z}X$, with atomic number Z and mass number A, are defined as:

$$\frac{d\sigma_i}{d\Omega}(\theta) = \frac{Y_i(\theta)}{N_C \times N_{TG} \times \Delta\Omega \times \varepsilon^i_{trk}(\theta)} \tag{6.1}$$

$$\frac{d\sigma_i}{dE_{kin}}(E_{kin}) = \frac{Y_i(E_{kin})}{N_C \times N_{TG} \times \Delta E_{kin} \times \varepsilon^i_{trk}(E_{kin})} \tag{6.2}$$

where Y_i is the number of reconstructed fragments for the i-th isotope in an angular or energy bin $\Delta\Omega$ or ΔE_{kin} respectively. N_C is the number of ^{12}C ions impinging on the target, provided by the SC, $N_{TG} = (\rho \times d \times N_a)/A$ where ρ and d are the target density and thickness respectively, while N_a and A are the Avogadro number and the target atomic mass respectively and ε^i_{trk} is the tracking reconstruction efficiency for the i-th isotope (defined in § 5).

The production abundance of each fragment (Y_i), as well as the identification of different isotopes for each charge hypothesis is measured using the reconstructed mass spectra. In order to compute properly the fragment yields Y_i the background has to be taken into account and subtracted. Two different components can be identified in the background mass spectra: the combinatorial background (see § 4) and a component coming from a wrong charge assignment from the Z_{ID} algorithm (see § 2.2) called "cross feed background". For a deeper explanation of the background subtraction procedure see [5].

In order to extract the fragment yield for each isotope ${}^{A}_{Z}X$, the reconstructed mass spectra are fitted, for each charge Z and for each angular and energy bin, taking into account a contribution from the signal and a contribution from the background.

The fragment yields Y_i are measured fitting the reconstructed mass spectra for each charge and angular (energy) bin, using an unbinned extended maximum likelihood approach, in which the signal and background yields are fitted together: the signal is modeled with a Gaussian PDF for each isotope and the background PDFs are extracted from the MC simulation (see [5]).

An example of mass fits, for fragments of different charges and for reconstructed mass spectra in different E_{kin} and θ bins, is shown in Fig. 5. Superimposed to the data distribution (black dots), the total PDF is shown (in red) while the signal PDF, modeling the various isotopes, is shown in blue. A magenta dotted line shows the contribution from the background PDF. The plot on the left shows the invariant mass fits to the H fragment spectra in a given bin of angle: protons, deuterons and tritons isotopes are clearly visible. The plot on the right shows the same information for Li fragments in different energy bins: the two visible peaks correspond to ^{6}Li and ^{7}Li isotopes; less visible is the ^{8}Li isotope.

The measured elemental differential cross sections, as a function of θ and E_{kin}, are shown in Figs. 6 respectively on the left and on the right. It can be noticed that while most of the fragments are forward emitted and with about the same kinetic energy of the ^{12}C beam, a not negligible fraction of the light Z = 1, 2 fragments are produced with larger angles and a wider kinetic energy distribution. As also expected from simulation (see [4]) the most of the emitted particles are fragments forward peaked, due to projectile fragmentation, with energies/nucleon and velocities

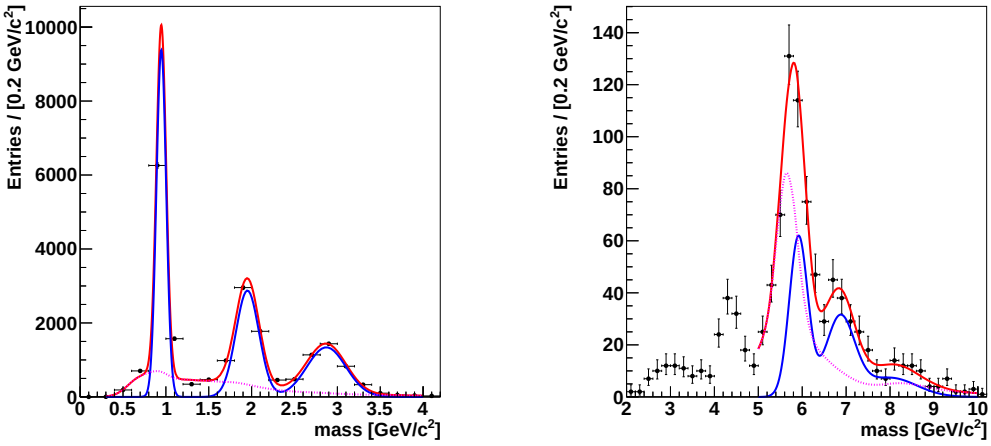

Figure 5: Mass fit results for H and Li fragments mass spectra. The plot on the left shows the invariant mass fits for H fragments with polar angles between 0.4° and 0.8°. The plot on the right shows the invariant mass fits for Li fragments with E_{kin} in the range between 260 MeV/nucleon and 290 MeV/nucleon.

distributed around the ^{12}C beam energy/nucleon. The contribution from target-fragments, isotropically distributed in the space, is expected to lower energies.

The $d\sigma/dE_{kin}$ results are referred to the ALADIN geometrical acceptance and have been unfolded to take into account the detector resolution. The unfolding procedure has been described in detail in [5].

The reported uncertainties account also for the systematic contribution, that dominates respect to the statistical one. The main contributions to the systematics are: 1-uncertainties due to the background PDF modeling and subtraction; 2-uncertainties due to local and global reconstruction algorithms; 3-uncertainties due to the detectors position and due to calibration and geometrical parameters. The main contribution is the one coming from the combinatorial background subtraction. A detailed explanation of the systematics study can be found in [5].

7. Conclusions

This paper has presented the analysis of the data collected with the FIRST apparatus for the measurement of the fragmentation cross sections in the interaction of a 400 MeV/nucleon ^{12}C beam on a thin (0.5 mm) gold target. The data collected at the SIS accelerator of the GSI laboratory have been analyzed to measure the fragmentation differential cross sections as a function of the emission angle θ and the kinetic energy E_{kin}. The present analysis was focused on the fragments emitted at angles $\theta \lesssim 6°$, in the angular acceptance of the ALADIN magnet. Here only the elemental cross sections have been shown. The fragmentation cross sections for the different isotopes produced in the interaction of carbon with gold have also been studied and reported in [5], together with a more accurate description of the analysis techniques used. The results presented here achieve an unprecedented precision on the fragmentation cross sections of ^{12}C ions on a gold target and can be evaluable benchmarking for the interaction nuclear models implemented in MC codes.

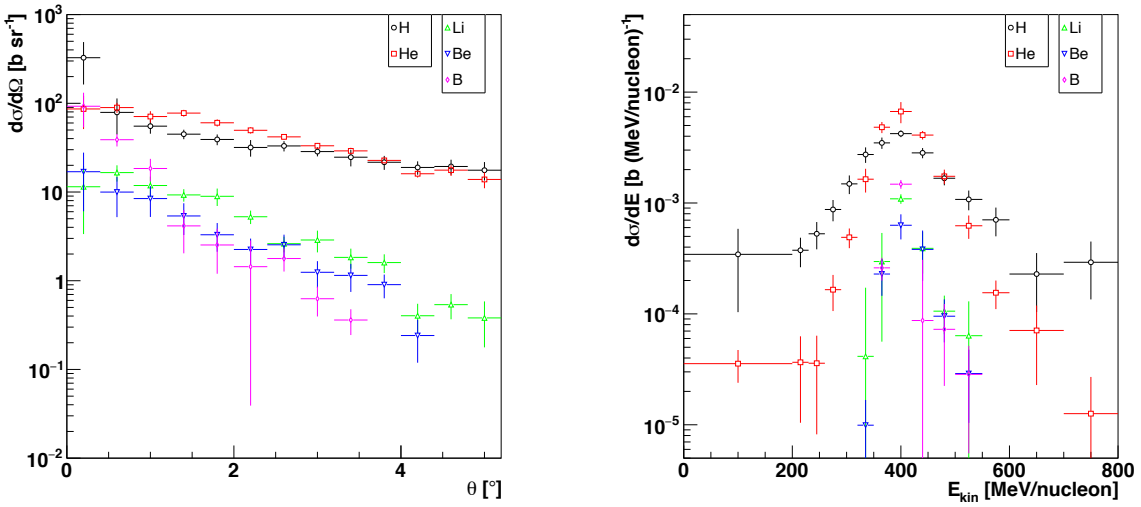

Figure 6: Left: Elemental differential cross sections as a function of the fragment angle with respect to the beam axis.The total uncertainty is shown: for most of the points is well below the marker size. Right: Elemental differential cross sections for the gold target, as a function of the fragment normalized kinetic energyfor fragments within the ALADIN angular acceptance ($\lesssim 6^{\circ}$). The total uncertainty is shown.

References

[1] M. Durante and J. S. Loeffler, *Charged particles in radiation oncology*, *Nat. Rev. Clin. Oncol.* **7**, 37-43, (2010).

[2] J. W. Norbury, J. Miller et al., *Review f Nuclear Physics Experiments for Space Radiation*, *NASA/TP-2011-217179*, (2011).

[3] T. T. Böhlen et al., *Benchmarking nuclear models of FLUKA and GEANT4 for carbon ion therapy*, *Physics in Medicine and Biology* **55**, 5833-5847, (2010).

[4] R. Pleskac et al., *The FIRST experiment at GSI*, *Nucl. Instrum. Methods Phys. Res. A*, **678**, 130-138, (2012).

[5] M. Toppi et.al., *Measurement of fragmentation cross sections of ^{12}C ions on a thin gold target with the FIRST apparatus*, *Phys. Rev. C*, **93**, 064601, (2016).

[6] Z. Abou-Haidar et al., *Performance of upstream interaction region detectors for the FIRST experiment at GSI*, *JINST*, **7**, P02006, (2012).

[7] R. Rescigno et al., *Performance of the reconstruction algorithms of the FIRST experiment pixel sensors vertex detector*, *Nucl. Instrum. Methods Phys. Res. A*, **767**, 34-40, (2014).

[8] C. Hu-Guo et al., *First reticule size MAPS with digital output and integrated zero suppression for the EUDET-JRA1 beam telescope*, *Nuclear Inst. and Methods in Physics Research*, **623**, 480-482, (2010.)

[9] A. Ferrari, P. R. Sala, A. Fassó, J. Ranft, *FLUKA: A Multi Particle Transport Code*, *Technical Report CERN-2005-10, INFN/TC05/11, SLAC-R-773*, (2005).